



# Hybrid model estimate of the ocean carbon sink from 1959 to 2022

Jens Terhaar<sup>1,2</sup>

<sup>1</sup>Climate and Environmental Physics, Physics Institute, University of Bern, Bern, Switzerland

<sup>2</sup>Oeschger Centre for Climate Change Research, University of Bern, Bern, Switzerland

5 *Correspondence to:* Jens Terhaar (jens.terhaar@unibe.ch)

**Abstract.** The ocean takes up around one quarter of anthropogenically emitted carbon and is projected to remain the main carbon sink once global temperatures stabilize. Despite the importance of this carbon sink, estimates of its strength over the last decades remain uncertain, mainly due to too few and unevenly sampled observations and shortcomings in ocean models and their setups. Here, I present a hybrid model estimate of the annually averaged ocean carbon sink from 1959 to 2022 by  
10 combining the higher-frequency variability of the annually averaged estimates of the carbon sink from ocean models in hindcast mode and the long-term trends from fully coupled Earth System Models. Ocean models in hindcast mode reproduce the observed climate variability, but their spin-up strategy likely leads to too weak long-term trends, whereas fully coupled Earth System Models simulate their own internal climate variability but better represent long-term trends. By combining these two modelling approaches, I keep the strength of each approach and remove the respective weaknesses. This hybrid  
15 model estimate of the ocean carbon sink from 1959 to 2022 is  $125 \pm 8$  Pg C and is similar in magnitude but 70% less uncertain than the best estimate of the Global Carbon Budget.

## 1 Introduction

The ocean is a major natural sink of anthropogenic carbon (Broecker et al., 1979; Sarmiento et al., 1992) and took up around  
20 one quarter of carbon emissions from fossil fuels and land use change over the last decades (Friedlingstein et al., 2023; Terhaar et al., 2022; Müller et al., 2023; DeVries et al., 2023). Moreover, the ocean will continue taking up carbon over the 21<sup>st</sup> century (Terhaar et al., 2022) and beyond when temperatures are eventually stabilizing (Silvy et al., 2024). Despite the importance of the ocean carbon sink for the global carbon cycle and hence the global climate, large uncertainties exist with respect to the magnitude, variability, and trends of the ocean carbon sink (DeVries et al., 2023; Terhaar et al., 2024;  
25 Friedlingstein et al., 2023).

Observation-based annually-resolved estimates of the ocean carbon sink are built on direct observations of the partial pressure of CO<sub>2</sub> ( $p\text{CO}_2$ ) at the ocean surface (Fay et al., 2021). While being built on observations is a strength of these observation-based  $p\text{CO}_2$  products, it is also their weakness. As observations are scarce in space and time, they must be  
30 extrapolated by methods relying among others on artificial intelligence and machine learning, for example neural networks



(Landschützer et al., 2015). However, even these cutting-edge extrapolation methods introduce biases in the strength of the decadal variability (Gloege et al., 2021) and trends (Hauck et al., 2023; Terhaar, 2024). The data scarcity and uneven spacing in the past is impossible to overcome and the question was raised if the different methods of extrapolating these observations have “hit the wall” (Gregor et al., 2019).

35

An alternative to observation-based  $p\text{CO}_2$  products are global ocean biogeochemical models (GOBMs) that are forced with historical atmospheric reanalysis data, atmospheric  $\text{CO}_2$ , and radiative forcing from other radiative agents. As GOBMs are forced with these historical data, they represent the observed internal climate variability at the ocean surface and hence the high-frequency variability of the annually averaged ocean carbon sink, i.e., inter-annual to sub-decadal variability. However, differences in the simulated carbon sink by GOBMs are caused by differences in the simulated circulation and carbonate chemistry in these models (Terhaar et al., 2024), as well as different ways of setting up these GOBMs, e.g., the lengths of the spin-up or different atmospheric  $\text{CO}_2$  during the pre-industrial spin-up (Terhaar et al., 2024). Moreover, using atmospheric forcing from sometime between 1959 and present, the period when atmospheric reanalysis data is provided, for the pre-industrial spin-up leads to a too warm pre-industrial ocean and hence too weak transient warming in GOBMs (Huguenin et al., 2022) and too weak deoxygenation (Takano et al., 2023). This too warm pre-industrial ocean and too weak ocean warming may also influence the ocean carbon sink and its trends through biases in the base state and transient changes in the stratification, solubility, or carbonate chemistry of the ocean. However, the sign and magnitude of that effect remains still unclear.

50 Another option to estimate the annually resolved ocean carbon sink are fully coupled Earth System Models (ESMs) that are also forced with historical atmospheric  $\text{CO}_2$  and radiative forcing from other radiative agents but dynamically simulate their atmosphere. Being dynamically coupled, ESMs do not simulate the phase of the observed internal climate variability and hence not the high-frequency variability of the annually averaged ocean carbon sink. However, ESMs from the most recent phase 6 of the coupled model intercomparison project (CMIP6) are all set up in a common way, having the same atmospheric  $\text{CO}_2$  during the pre-industrial spin-up and long enough spin-ups that allow the simulated ocean to reach its own equilibrium (Séférian et al., 2016). Furthermore, their pre-industrial atmospheric and ocean temperatures in ESMs are colder than their respective historical temperatures so that the simulated transient ocean warming aligns with observed ocean warming (Takano et al., 2023). Finally, the simulated global ocean carbon sink could be adjusted for their biases in the simulated ocean circulation and carbonate chemistry with observations (Terhaar et al., 2021, 2022). Thus, ESMs from CMIP6 can be considered to robustly simulate the long-term trends of the ocean carbon sink and the externally-forced decadal variability, which is mostly driven by changes in the atmospheric  $\text{CO}_2$  growth rate (Terhaar, 2024; McKinley et al., 2020).



As both model estimates will not overcome their respective weaknesses in the near future, I here propose a new hybrid  
65 model estimate of the ocean carbon sink combining the inter-annual and sub-decadal variability of the ocean carbon sink  
from GOBMs and the externally forced decadal variability and long-term evolution of the ocean carbon sink from ESMs.  
The combined estimate uses the strength and removes the weaknesses of the respective model estimates.

## 2 Results

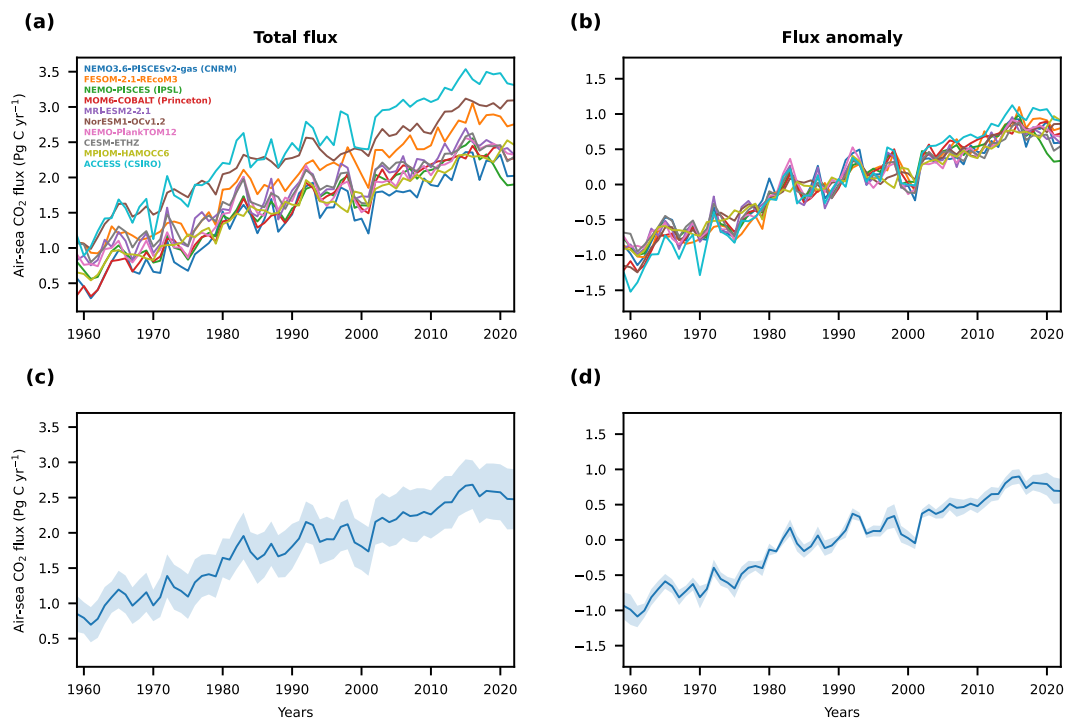
### 2.1 A new hybrid model estimate

70 The 10 GOBMs from the Global Carbon Budget 2023 simulate a global ocean carbon sink from 1959 to 2022 of various  
strengths (Friedlingstein et al., 2023) (Fig. 1a, c) but the flux anomaly with respect to the mean simulated carbon sink over  
the entire period is almost indistinguishable across these GOBMs (Fig. 1b, d). Small common differences in the anomalies  
exist in 1985 and 1998 for the GOBMs NorESM1-OCv1.2 (Schwinger et al., 2016) and MPIOM-HAMOCC6 (Lacroix et al.,  
2021b) (Fig. 1b), likely because both use the NCEP reanalysis data (Kanamitsu et al., 2002) to force the simulations and not  
75 the JRA55-do (Tsuji et al., 2018) or ERA5 reanalysis datasets (Hersbach et al., 2020) as the other simulations do.  
Furthermore, the ACCESS (CSIRO) model (Law et al., 2017) simulates slightly weaker anomalies at the beginning of the  
simulation and stronger anomalies at the end of the simulations resulting in a larger trend of the anomalies over the entire  
period (Fig. 1b), although the models set-up is not different to the others (Friedlingstein et al., 2023). Nevertheless, the  
overall strong agreement in simulated anomalies of the global ocean carbon sink across these 10 GOBMs as expressed by the  
80 small multi-model standard deviation leads to small uncertainties of the multi-model mean estimate of the high-frequency  
variability of the simulated global ocean carbon sink by GOBMs (Fig. 1d).

As there small inter-model differences in the simulated high-frequency variability of the global ocean carbon sink by the  
GOBMs and as it has been shown that ESMs largely agree in the magnitude and long-term trends of the global ocean carbon  
85 sink after adjusting for biases in ocean circulation and carbonate chemistry (Terhaar et al., 2022) and that the multi-model  
mean of ESMs can represent the externally forced decadal trends (Li and Ilyina, 2018; Terhaar, 2024), I here combine both  
model estimates to create a new hybrid model estimate of the global ocean carbon sink (Fig. 2c, Table A1). The high-  
frequency variability was here extracted by removing a spline fit (Enting, 1987) from the simulated carbon sink estimate  
from each GOBM separately (Friedlingstein et al., 2023) (Fig. 2b). The low-frequency variability and long-term trends were  
90 calculated by fitting a spline fit (Enting, 1987) to the bias-adjusted simulated carbon sink from each ESM separately  
(Terhaar et al., 2022) (Fig. 2a). The ESMs were forced with historical forcing until 2014 and with forcing from the Shared  
Socioeconomic Pathways 1-2.6 (SSP1-2.6) (Riahi et al., 2017) after 2014 as the atmospheric CO<sub>2</sub> under that SSP  
(Meinshausen et al., 2020) is closest but still slightly above the observed atmospheric CO<sub>2</sub> (Lan et al., 2024). The uncertainty  
of the hybrid estimate is the combination of the multi-model standard deviation of the high-frequency variability from



95 GOBMs and that of the long-term trends from ESMs, as well as the uncertainty from the spline fit (see Appendix for more details).



100 **Figure 1: Global ocean carbon sink and its anomaly as simulated by global ocean biogeochemical models.** The global ocean carbon sink as defined by the Global Carbon Budget 2023 (Friedlingstein et al., 2023) and (a) simulated by 10 global ocean biogeochemical models as well as (c) the multi-model mean and standard deviation. In addition, (b) the anomaly of the ocean carbon sink for the 10 global ocean biogeochemical models with respect to the mean flux from 1959 to 2022 in the respective GOBM, as well as (d) the multi-model mean and standard deviation of that anomaly are shown.

105 The ocean carbon sink estimated by this hybrid model estimate from 1959 to 2022 is  $125 \pm 8$  Pg C (Fig. 1c, Table A1). It increases from  $1.00 \pm 0.10$  Pg C yr<sup>-1</sup> in the 1960s to  $2.78 \pm 0.16$  Pg C yr<sup>-1</sup> in the 2010s. The increase of the ocean carbon sink slows down in the 1990s (decadal trend of  $0.10$  Pg C yr<sup>-1</sup> dec<sup>-1</sup>) and accelerates afterwards (decadal trends of  $0.55$  and  $0.56$  Pg C yr<sup>-1</sup> dec<sup>-1</sup> in the 2000s and 2010s) as expected from the trends in atmospheric CO<sub>2</sub> and the eruption of Mount Pinatubo in the early 1990s (McKinley et al., 2020; Fay et al., 2023; Terhaar, 2024).

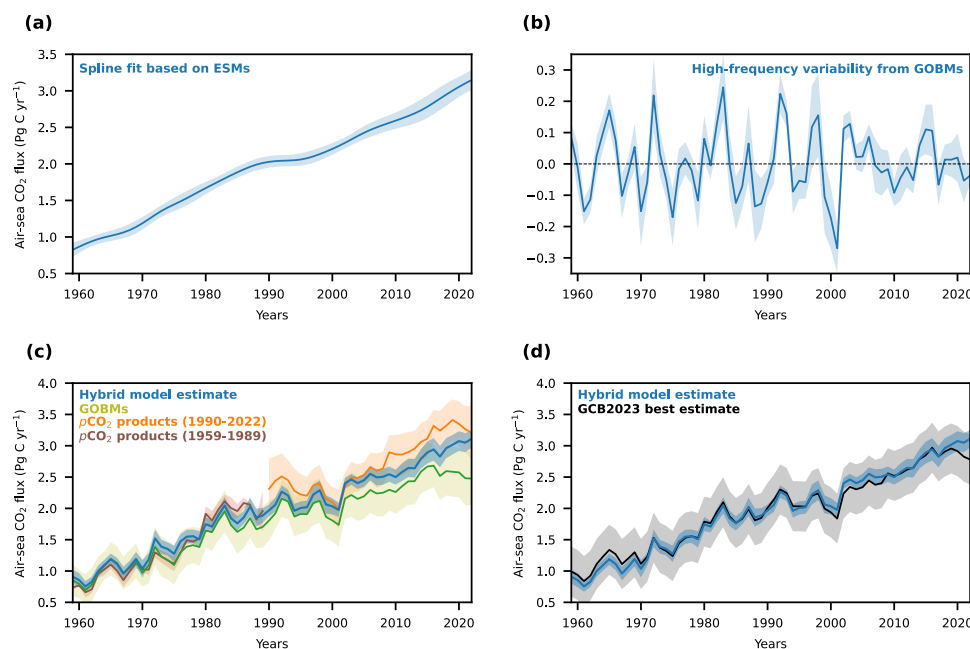


**Figure 2: Hybrid model estimate of the ocean carbon sink and its two components.** (a) A spline fit to the ocean carbon sink as simulated by ESMs from Earth System Models and adjusted for biases in the ocean circulation and carbonate chemistry (Terhaar et al., 2022) as well as (b) the high-frequency variability of the ocean carbon sink anomalies as simulated by GOBMs that was derived after removing a spline fit to the simulated anomalies. The multi-model mean estimates are shown as blue lines and the multi-model standard deviation as blue shading. (c) The hybrid estimate is then the sum of the timeseries in (a) and (b). The uncertainties of the hybrid model estimates are the combined uncertainties of (a) and (b) plus the uncertainty from the spline fit (see Appendix for details). In addition, estimates from the GOBMs (olive line and shading for multi-model mean and standard deviation) and the  $p\text{CO}_2$  products from the Global Carbon Budget 2023 (Friedlingstein et al., 2023) (orange lines and shading show the multi-product mean and standard deviations over 8  $p\text{CO}_2$  products from 1990 to 2022, brown lines show the shading for multi-product mean and standard deviation over 2  $p\text{CO}_2$  products from 1959 to 2021) are shown for comparison in (c) and the best estimate from the Global Carbon Budget 2023 (black line and shading for multi-model mean and uncertainty as reported in the Global Carbon Budget 2023) in (d).

## 2.2 Comparison to previous estimates of the global ocean carbon sink

The new hybrid model estimate of the global ocean carbon sink differs from previous estimates by  $p\text{CO}_2$  products and GOBMs in terms of magnitude, trend, and variability. The ocean carbon sink in the hybrid model estimate is 10% (11 Pg C) larger than the estimate from GOBMs for the period from 1959 to 2022 (Fig. A1a). The absolute difference between both estimates has some variability over time but remains on average the same until 2014. After 2014, the hybrid estimate becomes steadily larger until and the difference rises from 0.24 Pg C yr<sup>-1</sup> (8%) averaged from 2005 to 2014 to 0.65 Pg C yr<sup>-1</sup> (26%) in 2022 (Fig. A1a). The difference before 2014 is likely due to a bias in the GOBMs in their simulated circulation and carbonate chemistry (Terhaar et al., 2024) that also exists in ESMs but was corrected for (Terhaar et al., 2022). After 2014, the increasing difference may either be explained by slightly different trajectories of atmospheric CO<sub>2</sub> in ESMs under SSP1-



2.6 and the historical atmospheric CO<sub>2</sub>. Based on a previously identified relationship between changes in the trend of atmospheric CO<sub>2</sub> and trends in the ocean carbon sink (Terhaar, 2024), the trend in the ocean carbon sink in the ESMs from 2013 to 2022 is likely around 0.2 Pg C yr<sup>-1</sup> dec<sup>-1</sup> too large. The difference in the atmospheric CO<sub>2</sub> trajectory thus explains around half of the difference of both estimates after 2014. The other half might be due to biased transient warming caused by the spin-up strategy (Takano et al., 2023; Huguenin et al., 2022) and hence a bias in the evolution of the ocean carbon sink. However, to quantify such an effect, simulations with GOBMs following the spin-up strategy by Huguenin et al. (2022) would have to be performed.

Compared to *p*CO<sub>2</sub> products, the hybrid estimate of the global ocean carbon sink is only 3% (1 Pg C) larger for the period from 1959 and 1989 than the two *p*CO<sub>2</sub> products that provide estimates before 1990 and is 8% (7 Pg C) smaller than all 8 *p*CO<sub>2</sub> products on average for the period from 1990 to 2022 (Fig. A1b). The difference in the early 1990s and after 2000 might be due to overly strong decadal variability that has been shown to exist at least in one *p*CO<sub>2</sub> product (Gloege et al., 2021). This explanation is further supported by two further studies, one that showed that extrapolating unevenly spaced observations in space and time lead to overly strong trends in the estimates of the ocean carbon sink by *p*CO<sub>2</sub> products (Hauck et al., 2023) and one that used ESMs to show that the trends in *p*CO<sub>2</sub> products lies outside of what can be expected based on changes in the atmospheric CO<sub>2</sub> growth rate and climate variability (Terhaar, 2024). After 2019, the difference between the hybrid model estimate and the *p*CO<sub>2</sub> products decreases again, likely because of the above discussed difference in observed atmospheric CO<sub>2</sub> and the prescribed atmospheric CO<sub>2</sub> in ESMs after 2014 following SSP1-2.6.

The hybrid estimate is almost identical to the best estimate of the ocean carbon sink provided by the Global Carbon Budget 2023 (Fig. 2d), which represents the average of the estimate by GOBMs and the *p*CO<sub>2</sub> products. The hybrid estimate thus corroborates this best estimate by the Global Carbon Budget 2023. However, instead of simply averaging two independent estimates, the hybrid model estimate uses the best available knowledge to remove the weaknesses of each model estimate and to only keep the strengths. As the hybrid model estimate explains the differences, its uncertainty is around 70% smaller than that of the best estimate of the Global Carbon Budget 2023.

### 3 Conclusion

Overall, the hybrid model estimate of the global ocean carbon sink combines two so far mostly separated model classes and successfully manages to account for the shortcomings in the different global ocean carbon sink estimates, i.e., the low bias in GOBMs due to the spin-up and the representation of the ocean circulation and carbonate chemistry and the bias towards too large decadal variability and trends in the *p*CO<sub>2</sub> products. The same method could also be applied to derive hybrid model estimates of regional and monthly-resolved estimates of the ocean carbon sink.



Although this hybrid estimate provides an improvement to existing estimates of both model classes, GOBMs (Friedlingstein et al., 2023; DeVries et al., 2023) and ESMs (Terhaar et al., 2022), it still has shortcomings. One shortcoming is the forcing of ESMs with SSPs after 2014 that leads to slightly too high carbon sink estimates from 2015 to 2022. This shortcoming could be overcome if ESMs were run with observed atmospheric CO<sub>2</sub> after the historical forcing from CMIP6 ends in 2014.

170 Another shortcoming is that all ESMs start in 1850 and are spun-up with atmospheric CO<sub>2</sub>, which leads to an underestimation of the ocean carbon sink (Bronse laer et al., 2017) of around 0.05-0.10 Pg C yr<sup>-1</sup> for ESMs for the period from 1959 to 2022 (Terhaar et al., 2024). This underestimation could be removed if ESMs were to start before the industrial revolution and the associated increase in atmospheric CO<sub>2</sub>.

175 The need for a hybrid model estimate of the global ocean carbon arose due to shortcomings in both model classes. As ESMs will always simulate an internal climate variability in a different phase than the observed one, this estimate remains a necessary fix until GOBMs are set up so that they can overcome their current weaknesses. To overcome current weaknesses, I recommend testing if an improved spin-up strategy that accounts for the difference in atmospheric and surface ocean temperatures as well as radiation between the pre-industrial times and the mid 20<sup>th</sup> century, for example as proposed by

180 Huguenin et al. (2022), may explain differences in the trends of the ocean carbon sink between GOBMs and ESMs. Furthermore, previous suggestions provided by Terhaar et al. (2024), such as a long enough spin-up and an early starting date and an associated atmospheric CO<sub>2</sub> during the spin-up, will likely also improve the carbon sink estimates by GOBMs. Once GOBMs are set-up in a common way, emergent constraints could also be used in GOBMs to correct for biases in the ocean circulation and carbonate chemistry as it was done for ESMs regionally and globally (Goris et al., 2018; Terhaar et al.,

185 2021, 2022, 2020; Bourgeois et al., 2022; Vaittinada Ayar et al., 2022). Until then, the here provided hybrid model estimate of the global ocean annually averaged carbon sink circumvents these shortcomings in GOBMs at present with the help of ESMs and thus provides a robust estimate of the global ocean carbon from 1959 to 2022.



## 190 4 Appendix

### 4.1 Estimates of the ocean carbon sink

Estimates of the ocean carbon sink, defined as the change in the globally integrated air-sea CO<sub>2</sub> flux since pre-industrial times due to increasing CO<sub>2</sub> and climate change, from *p*CO<sub>2</sub> products, GOBMs, and ESMs was used. Estimates of the global ocean carbon sink were directly taken for 8 *p*CO<sub>2</sub> products (Table A2) and 10 GOBMs (Table A3) from the Global Carbon Budget 2023 (Friedlingstein et al., 2023) (<https://doi.org/10.18160/gcp-2023>). In addition, the best estimate from the Global Carbon Budget 2023 was also directly taken from <https://doi.org/10.18160/gcp-2023>. For ESMs, estimates of the ocean carbon sink were calculated for 14 ESMs under historical forcing until 2014 and SSP1-2.6 from 2015 to 2022 following Terhaar et al. (2022) (Table A4).

The carbon sink estimates from ESMs were adjusted for biases in each model's circulation and carbonate chemistry as described by Terhaar et al (2022). The same predictors as in Terhaar et al (2022) were used. For the target variable, however, I here did not use the ocean carbon sink estimates from 1997 to 2014 but the ocean carbon sink from 1959 to 2022, the period for which this new hybrid model estimate provides annual ocean carbon sink estimates. To calculate the adjustment factors, I here used SSP5-8.5 after 2014 for which 3 more ESMs provide output (Table A4) as the higher number of ESMs makes the fit between predictors and target variables more robust (*r*<sup>2</sup> decreases from 0.82 to 0.63 when only using the 14 ESMs that provide output for SSP1-2.6).

### 4.2 Separating high-frequency variability and long-term trends

The high-frequency variability and long-term trends of the annually averaged global carbon sink in ESMs and GOBMs were separated by fitting a spline following Enting (1987) to the respective ocean carbon sink estimate. The fit itself represents the long-term trends and decadal variability and the residual, the difference between the original time series and the spline fit, is the defined as the high-frequency variability. I here used an openly available python implementation of this spline fitting method ([https://github.com/friedrichs-repo/enting\\_spline](https://github.com/friedrichs-repo/enting_spline)) with a cut-off period of 15 years. The cut-off period describes the period where 50% of the signal is attenuated by the spline. 15 years was chosen so guarantee that all sub-decadal variability is removed from the original timeseries.

To test the sensitivity to the choice, a hybrid model estimate was also calculated using an 11-year running mean instead of an spline using Enting (1987) with a cut-off period of 15 years. The hybrid model estimate using the 11-year running mean is almost indistinguishable from the estimate using Enting (1987) with a cut-off period of 15 years but differs at the start of the



220 end of the timeseries (Fig. A2). The running mean flattens out at the ends of timeseries with strong trends because neither the smaller values before the beginning of the timeseries nor the potentially larger values after the end of the timeseries are included. Thus, I here decided to rely on the spline fit from Enting (1987).

225 The spline fit itself also comes with uncertainties due to the choice of the cutoff period. Here, I calculated the hybrid model estimate using cutoff periods from 10 to 20 years (Fig. A3). The resulting hybrid model estimate is insensitive to the choice of the cutoff period. This insensitivity shows that it is essential that the inter-annual variability is taken from the GOBMs and the long-term trends from the ESMs. The variability in between, however, can be taken from either GOBMs or ESMs as the decadal variability and trends of the ocean carbon sink are mainly driven by the change in the trends in atmospheric CO<sub>2</sub>, i.e., the growth rate of atmospheric CO<sub>2</sub> (McKinley et al., 2017, 2020; Fay et al., 2023; Terhaar, 2024), and other external forcing such as volcanoes (McKinley et al., 2020; Fay et al., 2023; Frölicher et al., 2013), which are prescribed in GOBMs and ESMs (until 2014) based on observations.

### 230 4.3 Uncertainty estimates

The uncertainties of the hybrid model estimate of the ocean carbon sink are a combination of the multi-model standard deviation of the high-frequency estimates from the GOBMs and the long-term trends from the ESMs, as well as the uncertainty from the choice of the cutoff period that was used to calculate the spline (Table A1). The uncertainty of the cutoff period was calculated as the standard deviation of all 11 estimates with cutoff periods from 10 to 20 years (Fig. A3). 235 The different uncertainties are added using error propagation, i.e., by calculating the square root of the sums of the squares of each uncertainty. The difference in the atmospheric CO<sub>2</sub> in the ESMs under SSP1-2.6 after 2014 was not explicitly added as an uncertainty but discussed as a caveat in the manuscript. All uncertainties are given as 1- $\sigma$ .



240

**Table A1: Annually averaged best estimates and uncertainties ( $1-\sigma$ ) of the global ocean carbon sink by the hybrid model estimate. All units are in  $\text{Pg C yr}^{-1}$ .**

| Year | Best estimate | Uncertainty<br>from GOBMs | Uncertainty<br>from ESMs | Uncertainty from<br>cutoff period | Combined uncertainty |
|------|---------------|---------------------------|--------------------------|-----------------------------------|----------------------|
| 1959 | 0.91          | 0.05                      | 0.10                     | 0.01                              | 0.11                 |
| 1960 | 0.85          | 0.08                      | 0.08                     | 0.01                              | 0.11                 |
| 1961 | 0.75          | 0.04                      | 0.07                     | 0.02                              | 0.09                 |
| 1962 | 0.83          | 0.04                      | 0.07                     | 0.02                              | 0.08                 |
| 1963 | 1.00          | 0.06                      | 0.07                     | 0.01                              | 0.09                 |
| 1964 | 1.09          | 0.05                      | 0.07                     | 0.01                              | 0.09                 |
| 1965 | 1.19          | 0.06                      | 0.07                     | 0.02                              | 0.09                 |
| 1966 | 1.11          | 0.06                      | 0.07                     | 0.02                              | 0.10                 |
| 1967 | 0.96          | 0.07                      | 0.08                     | 0.02                              | 0.11                 |
| 1968 | 1.07          | 0.05                      | 0.09                     | 0.02                              | 0.10                 |
| 1969 | 1.19          | 0.07                      | 0.09                     | 0.01                              | 0.12                 |
| 1970 | 1.04          | 0.11                      | 0.09                     | 0.00                              | 0.14                 |
| 1971 | 1.19          | 0.05                      | 0.08                     | 0.00                              | 0.10                 |
| 1972 | 1.52          | 0.12                      | 0.08                     | 0.01                              | 0.14                 |
| 1973 | 1.39          | 0.07                      | 0.08                     | 0.02                              | 0.11                 |
| 1974 | 1.35          | 0.06                      | 0.08                     | 0.02                              | 0.11                 |
| 1975 | 1.27          | 0.09                      | 0.09                     | 0.02                              | 0.13                 |
| 1976 | 1.47          | 0.06                      | 0.10                     | 0.02                              | 0.12                 |
| 1977 | 1.55          | 0.05                      | 0.10                     | 0.01                              | 0.11                 |
| 1978 | 1.56          | 0.05                      | 0.10                     | 0.00                              | 0.11                 |
| 1979 | 1.51          | 0.09                      | 0.09                     | 0.00                              | 0.13                 |
| 1980 | 1.75          | 0.07                      | 0.08                     | 0.01                              | 0.11                 |
| 1981 | 1.71          | 0.04                      | 0.08                     | 0.02                              | 0.09                 |
| 1982 | 1.89          | 0.07                      | 0.07                     | 0.03                              | 0.11                 |
| 1983 | 2.05          | 0.10                      | 0.07                     | 0.03                              | 0.13                 |
| 1984 | 1.84          | 0.10                      | 0.08                     | 0.01                              | 0.13                 |
| 1985 | 1.76          | 0.09                      | 0.08                     | 0.00                              | 0.12                 |
| 1986 | 1.85          | 0.07                      | 0.08                     | 0.02                              | 0.11                 |
| 1987 | 2.03          | 0.12                      | 0.08                     | 0.03                              | 0.15                 |
| 1988 | 1.85          | 0.12                      | 0.08                     | 0.03                              | 0.14                 |
| 1989 | 1.89          | 0.08                      | 0.08                     | 0.03                              | 0.12                 |
| 1990 | 1.97          | 0.05                      | 0.08                     | 0.02                              | 0.09                 |
| 1991 | 2.06          | 0.08                      | 0.08                     | 0.00                              | 0.11                 |
| 1992 | 2.27          | 0.06                      | 0.08                     | 0.01                              | 0.10                 |
| 1993 | 2.21          | 0.04                      | 0.08                     | 0.02                              | 0.09                 |
| 1994 | 1.96          | 0.07                      | 0.08                     | 0.03                              | 0.11                 |



|      |      |      |      |      |      |
|------|------|------|------|------|------|
| 1995 | 2.01 | 0.06 | 0.08 | 0.02 | 0.10 |
| 1996 | 2.02 | 0.05 | 0.09 | 0.02 | 0.10 |
| 1997 | 2.22 | 0.13 | 0.09 | 0.01 | 0.16 |
| 1998 | 2.29 | 0.13 | 0.09 | 0.00 | 0.16 |
| 1999 | 2.06 | 0.12 | 0.08 | 0.01 | 0.14 |
| 2000 | 2.03 | 0.10 | 0.08 | 0.02 | 0.13 |
| 2001 | 1.98 | 0.08 | 0.08 | 0.02 | 0.11 |
| 2002 | 2.40 | 0.04 | 0.08 | 0.01 | 0.09 |
| 2003 | 2.46 | 0.04 | 0.08 | 0.01 | 0.09 |
| 2004 | 2.40 | 0.04 | 0.08 | 0.01 | 0.09 |
| 2005 | 2.45 | 0.05 | 0.09 | 0.00 | 0.10 |
| 2006 | 2.55 | 0.04 | 0.10 | 0.01 | 0.10 |
| 2007 | 2.50 | 0.08 | 0.10 | 0.01 | 0.13 |
| 2008 | 2.50 | 0.07 | 0.10 | 0.01 | 0.13 |
| 2009 | 2.55 | 0.06 | 0.11 | 0.01 | 0.12 |
| 2010 | 2.50 | 0.04 | 0.11 | 0.01 | 0.12 |
| 2011 | 2.58 | 0.07 | 0.12 | 0.01 | 0.14 |
| 2012 | 2.65 | 0.06 | 0.13 | 0.01 | 0.15 |
| 2013 | 2.64 | 0.04 | 0.14 | 0.02 | 0.15 |
| 2014 | 2.79 | 0.04 | 0.15 | 0.03 | 0.16 |
| 2015 | 2.89 | 0.08 | 0.15 | 0.03 | 0.18 |
| 2016 | 2.94 | 0.08 | 0.16 | 0.02 | 0.18 |
| 2017 | 2.83 | 0.07 | 0.16 | 0.01 | 0.17 |
| 2018 | 2.96 | 0.05 | 0.15 | 0.00 | 0.16 |
| 2019 | 3.02 | 0.05 | 0.15 | 0.01 | 0.16 |
| 2020 | 3.07 | 0.08 | 0.14 | 0.01 | 0.16 |
| 2021 | 3.05 | 0.07 | 0.13 | 0.02 | 0.15 |
| 2022 | 3.11 | 0.03 | 0.14 | 0.02 | 0.14 |

245 **Table A2: Observation-based  $p\text{CO}_2$  products from the Global Carbon Budget 2023 (Friedlingstein et al., 2023).**

| $p\text{CO}_2$ product | Time period in GCB 2023 | References                                      |
|------------------------|-------------------------|-------------------------------------------------|
| CMEMS-LSCE-FFNNv2      | 1990-2022               | (Chau et al., 2022)                             |
| JMA-MLR                | 1990-2022               | (Iida et al., 2021)                             |
| LDEO-HPD               | 1959-2022               | (Gloeger et al., 2022; Bennington et al., 2022) |
| MPI-SOMFFN             | 1990-2022               | (Landschützer et al., 2016)                     |
| NIES-ML3               | 1990-2022               | (Zeng et al., 2022)                             |
| OS-ETHZ-GRaCER         | 1990-2022               | (Gregor and Gruber, 2021)                       |
| Jena-MLS               | 1959-2022               | (Rödenbeck et al., 2014, 2022)                  |
| UPEX-Watson            | 1990-2022               | (Watson et al., 2020)                           |



250 **Table A3: Global ocean biogeochemical models from the Global Carbon Budget 2023 (Friedlingstein et al., 2023).**

| Model name                   | References                                    |
|------------------------------|-----------------------------------------------|
| NEMO3.6-PISCESv2-gas (CNRM)  | (Berthet et al., 2019; Séférian et al., 2019) |
| FESOM-2.1-REcoM2             | (Gürses et al., 2023)                         |
| NEMO-PISCES (IPSL)           | (Aumont et al., 2015)                         |
| MOM6-COBALT (Princeton)      | (Liao et al., 2020)                           |
| MRI-ESM2-2                   | (Nakano et al., 2011; Urakawa et al., 2020)   |
| MICOM-HAMOCC (NorESM-OCv1.2) | (Schwinger et al., 2016)                      |
| NEMO-PlankTOM12              | (Wright et al., 2021)                         |
| CESM-ETHZ                    | (Doney et al., 2009)                          |
| MPIOM-HAMOCC6                | (Lacroix et al., 2021a)                       |
| ACCESS (CSIRO)               | (Law et al., 2017)                            |

**Table A4: List of Earth System Models that were used in this study.**

| Model name    | Available SSPs      | References                                   |
|---------------|---------------------|----------------------------------------------|
| ACCESS-ESM1-5 | SSP1-2.6 / SSP5-8.5 | (Ziehn et al., 2020)                         |
| CanESM5       | SSP1-2.6 / SSP5-8.5 | (Swart et al., 2019; Christian et al., 2022) |
| CanESM5-CanOE | SSP1-2.6 / SSP5-8.5 | (Swart et al., 2019; Christian et al., 2022) |
| CESM2         | SSP1-2.6 / SSP5-8.5 | (Danabasoglu et al., 2020)                   |
| CESM2-WACCM   | SSP1-2.6 / SSP5-8.5 | (Danabasoglu et al., 2020)                   |
| CMCC-ESM2     | SSP1-2.6 / SSP5-8.5 | (Lovato et al., 2022)                        |
| EC-Earth3-CC  | SSP5-8.5            | (Döscher et al., 2022)                       |
| GFDL-CM4      | SSP5-8.5            | (Held et al., 2019)                          |
| GFDL-ESM4     | SSP1-2.6 / SSP5-8.5 | (Dunne et al., 2020; Stock et al., 2020)     |
| IPSL-CM6A-LR  | SSP1-2.6 / SSP5-8.5 | (Boucher et al., 2020)                       |
| MIROC-ES2L    | SSP1-2.6 / SSP5-8.5 | (Hajima et al., 2020)                        |
| MPI-ESM1-2-HR | SSP1-2.6 / SSP5-8.5 | (Gutjahr et al., 2019)                       |
| MPI-ESM1-2-LR | SSP1-2.6 / SSP5-8.5 | (Mauritsen et al., 2019)                     |
| MRI-ESM2-0    | SSP5-8.5            | (Yukimoto et al., 2019)                      |
| NorESM2-LM    | SSP1-2.6 / SSP5-8.5 | (Tjiputra et al., 2020; Seland et al., 2020) |
| NorESM2-MM    | SSP1-2.6 / SSP5-8.5 | (Tjiputra et al., 2020; Seland et al., 2020) |
| UKESM1-0-LL   | SSP1-2.6 / SSP5-8.5 | (Sellar et al., 2020)                        |

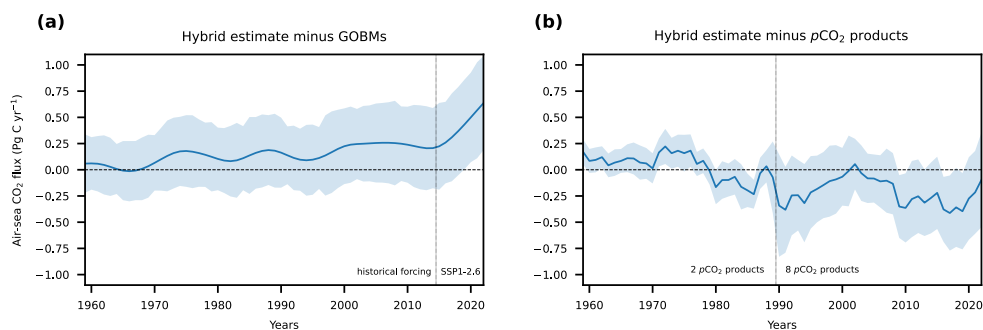
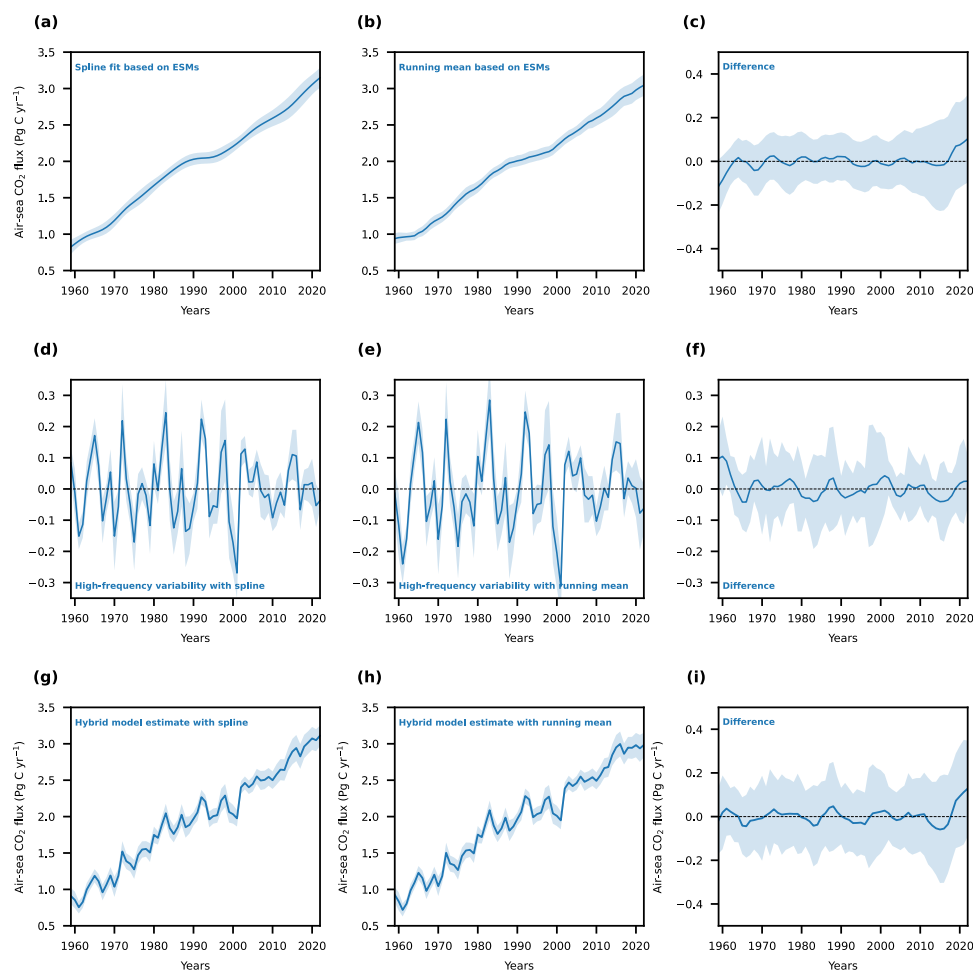


**Figure A1: Difference in estimates of the global ocean carbon sink between the new hybrid estimate and estimates from GOBMs and  $p\text{CO}_2$  products.** Difference between the hybrid estimate of the global ocean carbon sink and the estimates (a) from GOBMs and (b)  $p\text{CO}_2$  products from the Global Carbon Budget 2023 (Friedlingstein et al., 2023). The blue lines indicate the mean difference and the uncertainties show the combined uncertainties from the two respective estimates.



265 **Figure A2: Difference in estimates of the global ocean carbon sink between the new hybrid estimate and estimates from GOBMs and  $p\text{CO}_2$  products.** Difference between the hybrid estimate of the global ocean carbon sink and the estimates (a) from GOBMs and (b)  $p\text{CO}_2$  products from the Global Carbon Budget 2023 (Friedlingstein et al., 2023). The blue lines indicate the mean difference and the uncertainties show the combined uncertainties from the two respective estimates.

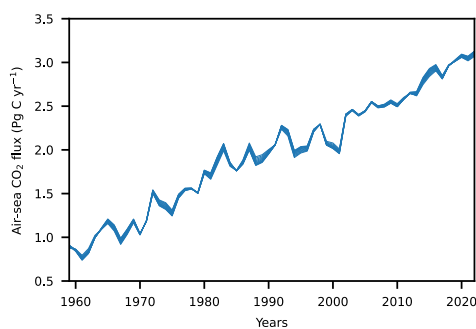


**Figure A3: The global ocean carbon sink estimate by the hybrid model estimate using different cutoff periods.** Each of the 11 lines here represents the global ocean carbon sink estimate by the hybrid model estimate using cutoff periods from 10 to 20 years.



### Data availability

280 The Earth system model output used in this study is available via the Earth System Grid Federation (<https://esgf-node.ipsl.upmc.fr/projects/esgf-ipsl/>, last access: 1 June 2022). The data from the Global Carbon Budget 2023 is available here (<https://doi.org/10.18160/gcp-2023>). The best estimate and uncertainties of the annually averaged estimate of the global carbon sink provided as estimated by the here presented hybrid model estimate are presented in table A1. If hybrid model estimate is too long for tables in other studies, please reference it as GOBM-ESM estimate.

### Competing interests

285 The author has declared that he has no competing interests.

### Acknowledgments

I thank Thomas L. Frölicher for helpful comments on the manuscript and the Swiss National Science Foundation for funding under grant # PZ00P2\_209044 (ArcticECO).

290



## References

- Aumont, O., Ethé, C., Tagliabue, A., Bopp, L., and Gehlen, M.: PISCES-v2: an ocean biogeochemical model for carbon and ecosystem studies, *Geosci. Model Dev.*, 8, 2465–2513, <https://doi.org/10.5194/gmd-8-2465-2015>, 2015.
- 295 Bennington, V., Gloege, L., and McKinley, G. A.: Observation-based variability in the global ocean carbon sink from 1959-2020, *Earth Sp. Sci. Open Arch.*, 14, <https://doi.org/10.1002/essoar.10510815.1>, 2022.
- Berthet, S., Séférian, R., Bricaud, C., Chevallier, M., Voldoire, A., and Ethé, C.: Evaluation of an Online Grid-Coarsening  
300 Algorithm in a Global Eddy-Admitting Ocean Biogeochemical Model, *J. Adv. Model. Earth Syst.*, 11, 1759–1783, <https://doi.org/10.1029/2019MS001644>, 2019.
- Boucher, O., Servonnat, J., Albright, A. L., Aumont, O., Balkanski, Y., Bastrikov, V., Bekki, S., Bonnet, R., Bony, S., Bopp, L., Braconnot, P., Brockmann, P., Cadule, P., Caubel, A., Cheruy, F., Codron, F., Cozic, A., Cugnet, D., D’Andrea, F.,  
305 Davini, P., de Lavergne, C., Denvil, S., Deshayes, J., Devilliers, M., Ducharne, A., Dufresne, J.-L., Dupont, E., Éthé, C., Fairhead, L., Falletti, L., Flavoni, S., Foujols, M.-A., Gardoll, S., Gastineau, G., Ghattas, J., Grandpeix, J.-Y., Guenet, B., Guez E., L., Guilyardi, E., Guimberteau, M., Hauglustaine, D., Hourdin, F., Idelkadi, A., Joussaume, S., Kageyama, M., Khodri, M., Krinner, G., Lebas, N., Levavasseur, G., Lévy, C., Li, L., Lott, F., Lurton, T., Luyssaert, S., Madec, G., Madeleine, J.-B., Maignan, F., Marchand, M., Marti, O., Mellul, L., Meurdesoif, Y., Mignot, J., Musat, I., Ottlé, C., Peylin, P., Planton, Y., Polcher, J., Rio, C., Rochetin, N., Rousset, C., Sepulchre, P., Sima, A., Swingedouw, D., Thiéblemont, R.,  
310 Traore, A. K., Vancoppenolle, M., Vial, J., Vialard, J., Viovy, N., and Vuichard, N.: Presentation and Evaluation of the IPSL-CM6A-LR Climate Model, *J. Adv. Model. Earth Syst.*, 12, e2019MS002010, <https://doi.org/10.1029/2019MS002010>, 2020.
- 315 Bourgeois, T., Goris, N., Schwinger, J., and Tjiputra, J. F.: Stratification constrains future heat and carbon uptake in the Southern Ocean between 30°S and 55°S, *Nat. Commun.*, 13, 340, <https://doi.org/10.1038/s41467-022-27979-5>, 2022.
- Broecker, W. S., Takahashi, T., Simpson, H. J., and Peng T.-H.: Fate of Fossil Fuel Carbon Dioxide and the Global Carbon Budget, *Science*, 206, 409–418, <https://doi.org/10.1126/science.206.4417.409>, 1979.
- 320 Bronselaer, B., Winton, M., Russell, J., Sabine, C. L., and Khatiwala, S.: Agreement of CMIP5 Simulated and Observed Ocean Anthropogenic CO<sub>2</sub> Uptake, *Geophys. Res. Lett.*, 44, 12, 212–298, 305,



<https://doi.org/https://doi.org/10.1002/2017GL074435>, 2017.

- 325 Chau, T. T. T., Gehlen, M., and Chevallier, F.: A seamless ensemble-based reconstruction of surface ocean  $p\text{CO}_2$  and air–sea  $\text{CO}_2$  fluxes over the global coastal and open oceans, 19, 1087–1109, <https://doi.org/10.5194/bg-19-1087-2022>, 2022.

- Christian, J. R., Denman, K. L., Hayashida, H., Holdsworth, A. M., Lee, W. G., Riche, O. G. J., Shao, A. E., Steiner, N., and Swart, N. C.: Ocean biogeochemistry in the Canadian Earth System Model version 5.0.3: CanESM5 and CanESM5-CanOE, 330 Geosci. Model Dev., 15, 4393–4424, <https://doi.org/10.5194/gmd-15-4393-2022>, 2022.

- Danabasoglu, G., Lamarque, J.-F., Bacmeister, J., Bailey, D. A., DuVivier, A. K., Edwards, J., Emmons, L. K., Fasullo, J., Garcia, R., Gettelman, A., Hannay, C., Holland, M. M., Large, W. G., Lauritzen, P. H., Lawrence, D. M., Lenaerts, J. T. M., Lindsay, K., Lipscomb, W. H., Mills, M. J., Neale, R., Oleson, K. W., Otto-Bliesner, B., Phillips, A. S., Sacks, W., Tilmes, 335 S., van Kampenhout, L., Vertenstein, M., Bertini, A., Dennis, J., Deser, C., Fischer, C., Fox-Kemper, B., Kay, J. E., Kinnison, D., Kushner, P. J., Larson, V. E., Long, M. C., Mickelson, S., Moore, J. K., Nienhouse, E., Polvani, L., Rasch, P. J., and Strand, W. G.: The Community Earth System Model Version 2 (CESM2), J. Adv. Model. Earth Syst., 12, <https://doi.org/https://doi.org/10.1029/2019MS001916>, 2020.

- 340 DeVries, T., Yamamoto, K., Wanninkhof, R., Gruber, N., Hauck, J., Müller, J. D., Bopp, L., Carroll, D., Carter, B. R., Chau, T. T. T., Doney, S. C., Gehlen, M., Gloege, L., Gregor, L., Henson, S., Kim, J. H., Iida, Y., Ilyina, T., Landschützer, P., Le Quéré, C., Munro, D. R., Nissen, C., Patara, L., Perez, F. F., Resplandy, L., Rodgers, K. B., Schwinger, J., Séférian, R., Sicardi, V., Terhaar, J., Triñanes, J., Tsujino, H., Watson, A. J., Yasunaka, S., and Zeng, J.: Magnitude, trends, and variability of the global ocean carbon sink from 1985–2018, Global Biogeochem. Cycles, 2023.

- 345 Doney, S. C., Lima, I., Feely, R. A., Glover, D. M., Lindsay, K., Mahowald, N., Moore, J. K., and Wanninkhof, R.: Mechanisms governing interannual variability in upper-ocean inorganic carbon system and air–sea  $\text{CO}_2$  fluxes: Physical climate and atmospheric dust, Deep Sea Res. Part II Top. Stud. Oceanogr., 56, 640–655, <https://doi.org/https://doi.org/10.1016/j.dsr2.2008.12.006>, 2009.

- 350 Döscher, R., Acosta, M., Alessandri, A., Anthoni, P., Arsouze, T., Bergman, T., Bernardello, R., Boussetta, S., Caron, L.-P., Carver, G., Castrillo, M., Catalano, F., Cvijanovic, I., Davini, P., Dekker, E., Doblas-Reyes, F. J., Docquier, D., Echevarria, P., Fladrich, U., Fuentes-Franco, R., Gröger, M., v. Hardenberg, J., Hieronymus, J., Karami, M. P., Keskinen, J.-P., Koenigk, T., Makkonen, R., Massonnet, F., Ménéguez, M., Miller, P. A., Moreno-Chamarro, E., Nieradzick, L., van Noije, T., Nolan, P., 355 O'Donnell, D., Ollinaho, P., van den Oord, G., Ortega, P., Prims, O. T., Ramos, A., Reerink, T., Rousset, C., Ruprich-Robert, Y., Le Sager, P., Schmith, T., Schrödner, R., Serva, F., Sicardi, V., Sloth Madsen, M., Smith, B., Tian, T., Tourigny,



E., Uotila, P., Vancoppenolle, M., Wang, S., Wårlind, D., Willén, U., Wyser, K., Yang, S., Yepes-Arbós, X., and Zhang, Q.: The EC-Earth3 Earth system model for the Coupled Model Intercomparison Project 6, *Geosci. Model Dev.*, 15, 2973–3020, <https://doi.org/10.5194/gmd-15-2973-2022>, 2022.

360

Dunne, J. P., Horowitz, L. W., Adcroft, A. J., Ginoux, P., Held, I. M., John, J. G., Krasting, J. P., Malyshev, S., Naik, V., Paulot, F., Shevliakova, E., Stock, C. A., Zadeh, N., Balaji, V., Blanton, C., Dunne, K. A., Dupuis, C., Durachta, J., Dussin, R., Gauthier, P. P. G., Griffies, S. M., Guo, H., Hallberg, R. W., Harrison, M., He, J., Hurlin, W., McHugh, C., Menzel, R., Milly, P. C. D., Nikonov, S., Paynter, D. J., Ploshay, J., Radhakrishnan, A., Rand, K., Reichl, B. G., Robinson, T., Schwarzkopf, D. M., Sentman, L. T., Underwood, S., Vahlenkamp, H., Winton, M., Wittenberg, A. T., Wyman, B., Zeng, Y., and Zhao, M.: The GFDL Earth System Model Version 4.1 (GFDL-ESM 4.1): Overall Coupled Model Description and Simulation Characteristics, *J. Adv. Model. Earth Syst.*, 12, e2019MS002015, <https://doi.org/https://doi.org/10.1029/2019MS002015>, 2020.

365

370 Enting, I. G.: On the use of smoothing splines to filter CO<sub>2</sub> data, *J. Geophys. Res. Atmos.*, 92, 10977–10984, <https://doi.org/https://doi.org/10.1029/JD092iD09p10977>, 1987.

Fay, A. R., Gregor, L., Landschützer, P., McKinley, G. A., Gruber, N., Gehlen, M., Iida, Y., Laruelle, G. G., Rödenbeck, C., Roobaert, A., and Zeng, J.: SeaFlux: harmonization of air–sea CO<sub>2</sub> fluxes from surface pCO<sub>2</sub> data products using a standardized approach, *Earth Syst. Sci. Data*, 13, 4693–4710, <https://doi.org/10.5194/essd-13-4693-2021>, 2021.

375

Fay, A. R., McKinley, G. A., Lovenduski, N. S., Eddebbar, Y., Levy, M. N., Long, M. C., Olivarez, H. C., and Rustagi, R. R.: Immediate and long-lasting impacts of the Mt. Pinatubo eruption on ocean oxygen and carbon inventories, *Global Biogeochem. Cycles*, n/a, e2022GB007513, <https://doi.org/https://doi.org/10.1029/2022GB007513>, 2023.

380

Friedlingstein, P., O’Sullivan, M., Jones, M. W., Andrew, R. M., Bakker, D. C. E., Hauck, J., Landschützer, P., Le Quéré, C., Luijkx, I. T., Peters, G. P., Peters, W., Pongratz, J., Schwingshackl, C., Sitch, S., Canadell, J. G., Ciais, P., Jackson, R. B., Alin, S. R., Anthoni, P., Barbero, L., Bates, N. R., Becker, M., Bellouin, N., Decharme, B., Bopp, L., Brasika, I. B. M., Cadule, P., Chamberlain, M. A., Chandra, N., Chau, T.-T.-T., Chevallier, F., Chini, L. P., Cronin, M., Dou, X., Enyo, K., Evans, W., Falk, S., Feely, R. A., Feng, L., Ford, D. J., Gasser, T., Ghattas, J., Gkritzalis, T., Grassi, G., Gregor, L., Gruber, N., Gürses, Ö., Harris, I., Hefner, M., Heinke, J., Houghton, R. A., Hurtt, G. C., Iida, Y., Ilyina, T., Jacobson, A. R., Jain, A., Jarníková, T., Jersild, A., Jiang, F., Jin, Z., Joos, F., Kato, E., Keeling, R. F., Kennedy, D., Klein Goldewijk, K., Knauer, J., Korsbakken, J. I., Körtzinger, A., Lan, X., Lefèvre, N., Li, H., Liu, J., Liu, Z., Ma, L., Marland, G., Mayot, N., McGuire, P. C., McKinley, G. A., Meyer, G., Morgan, E. J., Munro, D. R., Nakaoka, S.-I., Niwa, Y., O’Brien, K. M., Olsen, A., Omar, A. M., Ono, T., Paulsen, M., Pierrot, D., Pocock, K., Poulter, B., Powis, C. M., Rehder, G., Resplandy, L., Robertson, E.,

385

390



- Rödenbeck, C., Rosan, T. M., Schwinger, J., Séférian, R., et al.: Global Carbon Budget 2023, *Earth Syst. Sci. Data*, 15, 5301–5369, <https://doi.org/10.5194/essd-15-5301-2023>, 2023.
- Frölicher, T. L., Joos, F., Raible, C. C., and Sarmiento, J. L.: Atmospheric CO<sub>2</sub> response to volcanic eruptions: The role of ENSO, season, and variability, *Global Biogeochem. Cycles*, 27, 239–251, <https://doi.org/10.1002/gbc.20028>, 2013.
- Gloege, L., McKinley, G. A., Landschützer, P., Fay, A. R., Frölicher, T. L., Fyfe, J. C., Ilyina, T., Jones, S., Lovenduski, N. S., Rodgers, K. B., Schlunegger, S., and Takano, Y.: Quantifying Errors in Observationally Based Estimates of Ocean Carbon Sink Variability, *Global Biogeochem. Cycles*, 35, e2020GB006788, <https://doi.org/10.1029/2020GB006788>, 2021.
- Gloege, L., Yan, M., Zheng, T., and McKinley, G. A.: Improved Quantification of Ocean Carbon Uptake by Using Machine Learning to Merge Global Models and pCO<sub>2</sub> Data, *J. Adv. Model. Earth Syst.*, 14, e2021MS002620, <https://doi.org/10.1029/2021MS002620>, 2022.
- Goris, N., Tjiputra, J. F., Olsen, A., Schwinger, J., Lauvset, S. K., and Jeansson, E.: Constraining Projection-Based Estimates of the Future North Atlantic Carbon Uptake, *J. Clim.*, 31, 3959–3978, <https://doi.org/10.1175/JCLI-D-17-0564.1>, 2018.
- Gregor, L. and Gruber, N.: OceanSODA-ETHZ: a global gridded data set of the surface ocean carbonate system for seasonal to decadal studies of ocean acidification, *Earth Syst. Sci. Data*, 13, 777–808, <https://doi.org/10.5194/essd-13-777-2021>, 2021.
- Gregor, L., Lebehot, A. D., Kok, S., and Scheel Monteiro, P. M.: A comparative assessment of the uncertainties of global surface ocean CO<sub>2</sub> estimates using a machine-learning ensemble (CSIR-ML6 version2019a) – have we hit the wall?, *Geosci. Model Dev.*, 12, 5113–5136, <https://doi.org/10.5194/gmd-12-5113-2019>, 2019.
- Gürses, Ö., Oziel, L., Karakus, O., Sidorenko, D., Völker, C., Ye, Y., Zeising, M., and Hauck, J.: Ocean biogeochemistry in the coupled ocean-sea ice-biogeochemistry model FESOM2.1-REcoM3, *Geosci. Model Dev. Discuss.*, 2023, 1–73, <https://doi.org/10.5194/gmd-2023-2>, 2023.
- Gutjahr, O., Putrasahan, D., Lohmann, K., JungCLAUS, J. H., von Storch, J.-S., Brüggemann, N., Haak, H., and Stössel, A.: Max Planck Institute Earth System Model (MPI-ESM1.2) for the High-Resolution Model Intercomparison Project (HighResMIP), *Geosci. Model Dev.*, 12, 3241–3281, <https://doi.org/10.5194/gmd-12-3241-2019>, 2019.



425

Hajima, T., Watanabe, M., Yamamoto, A., Tatebe, H., Noguchi, M. A., Abe, M., Ohgaito, R., Ito, A., Yamazaki, D., Okajima, H., Ito, A., Takata, K., Ogochi, K., Watanabe, S., and Kawamiya, M.: Development of the MIROC-ES2L Earth system model and the evaluation of biogeochemical processes and feedbacks, *Geosci. Model Dev.*, 13, 2197–2244, <https://doi.org/10.5194/gmd-13-2197-2020>, 2020.

430

Hauck, J., Nissen, C., Landschützer, P., Rödenbeck, C., Bushinsky, S., and Olsen, A.: Sparse observations induce large biases in estimates of the global ocean CO<sub>2</sub> sink: an ocean model subsampling experiment, *Philos. Trans. R. Soc. A Math. Phys. Eng. Sci.*, 381, 20220063, <https://doi.org/10.1098/rsta.2022.0063>, 2023.

435

Held, I. M., Guo, H., Adcroft, A., Dunne, J. P., Horowitz, L. W., Krasting, J., Shevliakova, E., Winton, M., Zhao, M., Bushuk, M., Wittenberg, A. T., Wyman, B., Xiang, B., Zhang, R., Anderson, W., Balaji, V., Donner, L., Dunne, K., Durachta, J., Gauthier, P. P. G., Ginoux, P., Golaz, J.-C., Griffies, S. M., Hallberg, R., Harris, L., Harrison, M., Hurlin, W., John, J., Lin, P., Lin, S.-J., Malyshev, S., Menzel, R., Milly, P. C. D., Ming, Y., Naik, V., Paynter, D., Paulot, F., Ramaswamy, V., Reichl, B., Robinson, T., Rosati, A., Seman, C., Silvers, L. G., Underwood, S., and Zadeh, N.: Structure and Performance of GFDL's CM4.0 Climate Model, *J. Adv. Model. Earth Syst.*, 11, 3691–3727, <https://doi.org/https://doi.org/10.1029/2019MS001829>, 2019.

440

Hersbach, H., Bell, B., Berrisford, P., Hirahara, S., Horányi, A., Muñoz-Sabater, J., Nicolas, J., Peubey, C., Radu, R., Schepers, D., Simmons, A., Soci, C., Abdalla, S., Abellan, X., Balsamo, G., Bechtold, P., Biavati, G., Bidlot, J., Bonavita, M., De Chiara, G., Dahlgren, P., Dee, D., Diamantakis, M., Dragani, R., Flemming, J., Forbes, R., Fuentes, M., Geer, A., Haimberger, L., Healy, S., Hogan, R. J., Hólm, E., Janisková, M., Keeley, S., Laloyaux, P., Lopez, P., Lupu, C., Radnoti, G., de Rosnay, P., Rozum, I., Vamborg, F., Villaume, S., and Thépaut, J.-N.: The ERA5 global reanalysis, *Q. J. R. Meteorol. Soc.*, 146, 1999–2049, <https://doi.org/https://doi.org/10.1002/qj.3803>, 2020.

445

450

Huguenin, M. F., Holmes, R. M., and England, M. H.: Drivers and distribution of global ocean heat uptake over the last half century, *Nat. Commun.*, 13, 4921, <https://doi.org/10.1038/s41467-022-32540-5>, 2022.

455

Iida, Y., Takatani, Y., Kojima, A., and Ishii, M.: Global trends of ocean CO<sub>2</sub> sink and ocean acidification: an observation-based reconstruction of surface ocean inorganic carbon variables, *J. Oceanogr.*, 77, 323–358, <https://doi.org/10.1007/s10872-020-00571-5>, 2021.

Kanamitsu, M., Ebisuzaki, W., Woollen, J., Yang, S.-K., Hnilo, J. J., Fiorino, M., and Potter, G. L.: NCEP–DOE AMIP-II Reanalysis (R-2), *Bull. Am. Meteorol. Soc.*, 83, 1631–1644, <https://doi.org/https://doi.org/10.1175/BAMS-83-11-1631>,



2002.

460

Lacroix, F., Ilyina, T., Mathis, M., Laruelle, G. G., and Regnier, P.: Historical increases in land-derived nutrient inputs may alleviate effects of a changing physical climate on the oceanic carbon cycle, *Glob. Chang. Biol.*, 27, 5491–5513, <https://doi.org/https://doi.org/10.1111/gcb.15822>, 2021a.

465 Lacroix, F., Ilyina, T., Laruelle, G. G., and Regnier, P.: Reconstructing the Preindustrial Coastal Carbon Cycle Through a Global Ocean Circulation Model: Was the Global Continental Shelf Already Both Autotrophic and a CO<sub>2</sub> Sink?, *Global Biogeochem. Cycles*, 35, e2020GB006603, <https://doi.org/https://doi.org/10.1029/2020GB006603>, 2021b.

Lan, X., Tans, P., and Thoning, K. W.: Trends in globally-averaged CO<sub>2</sub> determined from NOAA Global Monitoring Laboratory measurements. Version 2024-05, NOAA Gml, <https://doi.org/https://doi.org/10.15138/9N0H-ZH07>, 2024.

Landschützer, P., Gruber, N., Haumann, F. A., Rödenbeck, C., Bakker, D. C. E., van Heuven, S., Hoppema, M., Metzl, N., Sweeney, C., Takahashi, T., Tilbrook, B., and Wanninkhof, R.: The reinvigoration of the Southern Ocean carbon sink, *Science*, 349, 1221–1224, <https://doi.org/10.1126/science.aab2620>, 2015.

475

Landschützer, P., Gruber, N., and Bakker, D. C. E.: Decadal variations and trends of the global ocean carbon sink, *Global Biogeochem. Cycles*, 30, 1396–1417, <https://doi.org/https://doi.org/10.1002/2015GB005359>, 2016.

Law, R. M., Ziehn, T., Matear, R. J., Lenton, A., Chamberlain, M. A., Stevens, L. E., Wang, Y.-P., Srbinovsky, J., Bi, D., Yan, H., and Vohralik, P. F.: The carbon cycle in the Australian Community Climate and Earth System Simulator (ACCESS-ESM1) -- Part 1: Model description and pre-industrial simulation, *Geosci. Model Dev.*, 10, 2567–2590, <https://doi.org/10.5194/gmd-10-2567-2017>, 2017.

Li, H. and Ilyina, T.: Current and Future Decadal Trends in the Oceanic Carbon Uptake Are Dominated by Internal Variability, *Geophys. Res. Lett.*, 45, 916–925, <https://doi.org/https://doi.org/10.1002/2017GL075370>, 2018.

Liao, E., Resplandy, L., Liu, J., and Bowman, K. W.: Amplification of the Ocean Carbon Sink During El Niños: Role of Poleward Ekman Transport and Influence on Atmospheric CO<sub>2</sub>, *Global Biogeochem. Cycles*, 34, e2020GB006574, <https://doi.org/https://doi.org/10.1029/2020GB006574>, 2020.

490

Lovato, T., Peano, D., Butenschön, M., Materia, S., Iovino, D., Scoccimarro, E., Fogli, P. G., Cherchi, A., Bellucci, A., Gualdi, S., Masina, S., and Navarra, A.: CMIP6 Simulations With the CMCC Earth System Model (CMCC-ESM2), *J. Adv.*



Model. Earth Syst., 14, e2021MS002814, <https://doi.org/https://doi.org/10.1029/2021MS002814>, 2022.

- 495 Mauritsen, T., Bader, J., Becker, T., Behrens, J., Bittner, M., Brokopf, R., Brovkin, V., Claussen, M., Crueger, T., Esch, M., Fast, I., Fiedler, S., Fläschner, D., Gayler, V., Giorgetta, M., Goll, D. S., Haak, H., Hagemann, S., Hedemann, C., Hohenegger, C., Ilyina, T., Jahns, T., Jimenéz-de-la-Cuesta, D., Jungclaus, J., Kleinen, T., Kloster, S., Kracher, D., Kinne, S., Kleberg, D., Lasslop, G., Kornbluh, L., Marotzke, J., Matei, D., Meraner, K., Mikolajewicz, U., Modali, K., Möbis, B., Müller, W. A., Nabel, J. E. M. S., Nam, C. C. W., Notz, D., Nyawira, S.-S., Paulsen, H., Peters, K., Pincus, R., Pohlmann, H., Pongratz, J., Popp, M., Raddatz, T. J., Rast, S., Redler, R., Reick, C. H., Rohrschneider, T., Schemann, V., Schmidt, H., Schnur, R., Schulzweida, U., Six, K. D., Stein, L., Stemmler, I., Stevens, B., von Storch, J.-S., Tian, F., Voigt, A., Vrese, P., Wieners, K.-H., Wilkenskjaeld, S., Winkler, A., and Roeckner, E.: Developments in the MPI-M Earth System Model version 1.2 (MPI-ESM1.2) and Its Response to Increasing CO<sub>2</sub>, *J. Adv. Model. Earth Syst.*, 11, 998–1038, <https://doi.org/https://doi.org/10.1029/2018MS001400>, 2019.
- 500
- McKinley, G. A., Fay, A. R., Lovenduski, N. S., and Pilcher, D. J.: Natural Variability and Anthropogenic Trends in the Ocean Carbon Sink, *Ann. Rev. Mar. Sci.*, 9, 125–150, <https://doi.org/10.1146/annurev-marine-010816-060529>, 2017.
- McKinley, G. A., Fay, A. R., Eddebbar, Y. A., Gloege, L., and Lovenduski, N. S.: External Forcing Explains Recent
- 510 Decadal Variability of the Ocean Carbon Sink, *AGU Adv.*, 1, e2019AV000149, <https://doi.org/https://doi.org/10.1029/2019AV000149>, 2020.
- Meinshausen, M., Nicholls, Z. R. J., Lewis, J., Gidden, M. J., Vogel, E., Freund, M., Beyerle, U., Gessner, C., Nauels, A., Bauer, N., Canadell, J. G., Daniel, J. S., John, A., Krummel, P. B., Luderer, G., Meinshausen, N., Montzka, S. A., Rayner, P. J., Reimann, S., Smith, S. J., van den Berg, M., Velders, G. J. M., Vollmer, M. K., and Wang, R. H. J.: The shared socio-economic pathway (SSP) greenhouse gas concentrations and their extensions to 2500, *Geosci. Model Dev.*, 13, 3571–3605, <https://doi.org/10.5194/gmd-13-3571-2020>, 2020.
- 515
- Müller, J. D., Gruber, N., Carter, B., Feely, R., Ishii, M., Lange, N., Lauvset, S. K., Murata, A., Olsen, A., Pérez, F. F., Sabine, C., Tanhua, T., Wanninkhof, R., and Zhu, D.: Decadal Trends in the Oceanic Storage of Anthropogenic Carbon From 1994 to 2014, *AGU Adv.*, 4, e2023AV000875, <https://doi.org/https://doi.org/10.1029/2023AV000875>, 2023.
- 520
- Nakano, H., Tsujino, H., Hirabara, M., Yasuda, T., Motoi, T., Ishii, M., and Yamanaka, G.: Uptake mechanism of anthropogenic CO<sub>2</sub> in the Kuroshio Extension region in an ocean general circulation model, *J. Oceanogr.*, 67, 765–783, <https://doi.org/10.1007/s10872-011-0075-7>, 2011.
- 525



- Riahi, K., van Vuuren, D. P., Kriegler, E., Edmonds, J., O'Neill, B. C., Fujimori, S., Bauer, N., Calvin, K., Dellink, R., Fricko, O., Lutz, W., Popp, A., Cuaresma, J. C., KC, S., Leimbach, M., Jiang, L., Kram, T., Rao, S., Emmerling, J., Ebi, K., Hasegawa, T., Havlik, P., Humpenöder, F., Da Silva, L. A., Smith, S., Stehfest, E., Bosetti, V., Eom, J., Gernaat, D., Masui, T., Rogelj, J., Strefler, J., Drouet, L., Krey, V., Luderer, G., Harmsen, M., Takahashi, K., Baumstark, L., Doelman, J. C., Kainuma, M., Klimont, Z., Marangoni, G., Lotze-Campen, H., Obersteiner, M., Tabeau, A., and Tavoni, M.: The Shared Socioeconomic Pathways and their energy, land use, and greenhouse gas emissions implications: An overview, *Glob. Environ. Chang.*, 42, 153–168, <https://doi.org/https://doi.org/10.1016/j.gloenvcha.2016.05.009>, 2017.
- 530 Rödenbeck, C., Bakker, D. C. E., Metzl, N., Olsen, A., Sabine, C., Cassar, N., Reum, F., Keeling, R. F., and Heimann, M.: Interannual sea–air CO<sub>2</sub> flux variability from an observation-driven ocean mixed-layer scheme, 11, 4599–4613, <https://doi.org/10.5194/bg-11-4599-2014>, 2014.
- Rödenbeck, C., DeVries, T., Hauck, J., Le Quéré, C., and Keeling, R. F.: Data-based estimates of interannual sea-air CO<sub>2</sub> flux variations 1957–2020 and their relation to environmental drivers, 19, 2627–2652, <https://doi.org/10.5194/bg-19-2627-2022>, 2022.
- 540 Sarmiento, J. L., Orr, J. C., and Siegenthaler, U.: A perturbation simulation of CO<sub>2</sub> uptake in an ocean general circulation model, *J. Geophys. Res. Ocean.*, 97, 3621–3645, <https://doi.org/https://doi.org/10.1029/91JC02849>, 1992.
- 545 Schwinger, J., Goris, N., Tjiputra, J. F., Kriest, I., Bentsen, M., Bethke, I., Ilicak, M., Assmann, K. M., and Heinze, C.: Evaluation of NorESM-OC (versions~1 and 1.2), the ocean carbon-cycle stand-alone configuration of the Norwegian Earth System Model (NorESM1), *Geosci. Model Dev.*, 9, 2589–2622, <https://doi.org/10.5194/gmd-9-2589-2016>, 2016.
- 550 Séférian, R., Gehlen, M., Bopp, L., Resplandy, L., Orr, J. C., Marti, O., Dunne, J. P., Christian, J. R., Doney, S. C., Ilyina, T., Lindsay, K., Halloran, P. R., Heinze, C., Segsneider, J., Tjiputra, J., Aumont, O., and Romanou, A.: Inconsistent strategies to spin up models in CMIP5: implications for ocean biogeochemical model performance assessment, *Geosci. Model Dev.*, 9, 1827–1851, <https://doi.org/10.5194/gmd-9-1827-2016>, 2016.
- 555 Séférian, R., Nabat, P., Michou, M., Saint-Martin, D., Voldoire, A., Colin, J., Decharme, B., Delire, C., Berthet, S., Chevallier, M., Sénési, S., Franchisteguy, L., Vial, J., Mallet, M., Joetzjer, E., Geoffroy, O., Guérémy, J.-F., Moine, M.-P., Msadek, R., Ribes, A., Rocher, M., Roehrig, R., Salas-y-Méla, D., Sanchez, E., Terray, L., Valcke, S., Waldman, R., Aumont, O., Bopp, L., Deshayes, J., Éthé, C., and Madec, G.: Evaluation of CNRM Earth System Model, CNRM-ESM2-1: Role of Earth System Processes in Present-Day and Future Climate, *J. Adv. Model. Earth Syst.*, 11, 4182–4227, <https://doi.org/https://doi.org/10.1029/2019MS001791>, 2019.
- 560



- Seland, Ø., Bentsen, M., Olivié, D., Toniazzi, T., Gjermundsen, A., Graff, L. S., Debernard, J. B., Gupta, A. K., He, Y.-C., Kirkevåg, A., Schwinger, J., Tjiputra, J., Aas, K. S., Bethke, I., Fan, Y., Griesfeller, J., Grini, A., Guo, C., Ilicak, M., Karset, I. H. H., Landgren, O., Liakka, J., Moseid, K. O., Nummelin, A., Spensberger, C., Tang, H., Zhang, Z., Heinze, C., Iversen, T., and Schulz, M.: Overview of the Norwegian Earth System Model (NorESM2) and key climate response of CMIP6 DECK, historical, and scenario simulations, *Geosci. Model Dev.*, 13, 6165–6200, <https://doi.org/10.5194/gmd-13-6165-2020>, 2020.
- Sellar, A. A., Walton, J., Jones, C. G., Wood, R., Abraham, N. L., Andrejczuk, M., Andrews, M. B., Andrews, T., Archibald, A. T., de Mora, L., Dyson, H., Elkinington, M., Ellis, R., Florek, P., Good, P., Gohar, L., Haddad, S., Hardiman, S. C., Hogan, E., Iwi, A., Jones, C. D., Johnson, B., Kelley, D. I., Kettleborough, J., Knight, J. R., Köhler, M. O., Kuhlbrodt, T., Liddicoat, S., Linova-Pavlova, I., Mizielinski, M. S., Morgenstern, O., Mulcahy, J., Neining, E., O'Connor, F. M., Petrie, R., Ridley, J., Rioual, J.-C., Roberts, M., Robertson, E., Rumbold, S., Seddon, J., Shepherd, H., Shim, S., Stephens, A., Teixeira, J. C., Tang, Y., Williams, J., Wiltshire, A., and Griffiths, P. T.: Implementation of U.K. Earth System Models for CMIP6, *J. Adv. Model. Earth Syst.*, 12, e2019MS001946, <https://doi.org/https://doi.org/10.1029/2019MS001946>, 2020.
- Silvy, Y., Frölicher, T. L., Terhaar, J., Joos, F., Burger, F. A., Lacroix, F., Allen, M., Bernadello, R., Bopp, L., Brovkin, V., Buzan, J. R., Cadule, P., Dix, M., Dunne, J., Friedlingstein, P., Georgievski, G., Hajima, T., Jenkins, S., Kawamiya, M., Kiang, N. Y., Lapin, V., Lee, D., Lerner, P., Mengis, N., Monteiro, E. A., Paynter, D., Peters, G. P., Romanou, A., Schwinger, J., Sparrow, S., Stofferahn, E., Tjiputra, J., Tourigny, E., and Ziehn, T.: AERA-MIP: Emission pathways, remaining budgets and carbon cycle dynamics compatible with 1.5°C and 2°C global warming stabilization, 2024, 1–47, <https://doi.org/10.5194/egusphere-2024-488>, 2024.
- Stock, C. A., Dunne, J. P., Fan, S., Ginoux, P., John, J., Krasting, J. P., Laufkötter, C., Paulot, F., and Zadeh, N.: Ocean Biogeochemistry in GFDL's Earth System Model 4.1 and Its Response to Increasing Atmospheric CO<sub>2</sub>, *J. Adv. Model. Earth Syst.*, 12, <https://doi.org/https://doi.org/10.1029/2019MS002043>, 2020.
- Swart, N. C., Cole, J. N. S., Kharin, V. V., Lazare, M., Scinocca, J. F., Gillett, N. P., Anstey, J., Arora, V., Christian, J. R., Hanna, S., Jiao, Y., Lee, W. G., Majaess, F., Saenko, O. A., Seiler, C., Seinen, C., Shao, A., Sigmond, M., Solheim, L., von Salzen, K., Yang, D., and Winter, B.: The Canadian Earth System Model version 5 (CanESM5.0.3), *Geosci. Model Dev.*, 12, 4823–4873, <https://doi.org/10.5194/gmd-12-4823-2019>, 2019.
- Takano, Y., Ilyina, T., Tjiputra, J., Eddebbar, Y. A., Berthet, S., Bopp, L., Buitenhuis, E., Butenschön, M., Christian, J. R., Dunne, J. P., Gröger, M., Hayashida, H., Hieronymus, J., Koenigk, T., Krasting, J. P., Long, M. C., Lovato, T., Nakano, H.,



595 Palmieri, J., Schwinger, J., Séférian, R., Suntharalingam, P., Tatebe, H., Tsujino, H., Urakawa, S., Watanabe, M., and Yool, A.: Simulations of ocean deoxygenation in the historical era: insights from forced and coupled models, *Front. Mar. Sci.*, 10, 2023.

Terhaar, J.: Drivers of decadal trends of the ocean carbon sink in the past, present, and future in Earth system models, 2024, 600 1–43, <https://doi.org/10.5194/egusphere-2024-773>, 2024.

Terhaar, J., Kwiatkowski, L., and Bopp, L.: Emergent constraint on Arctic Ocean acidification in the twenty-first century, *Nature*, 582, 379–383, <https://doi.org/10.1038/s41586-020-2360-3>, 2020.

605 Terhaar, J., Frölicher, T., and Joos, F.: Southern Ocean anthropogenic carbon sink constrained by sea surface salinity, *Sci. Adv.*, 7, 5964–5992, <https://doi.org/10.1126/sciadv.abd5964>, 2021.

Terhaar, J., Frölicher, T. L., and Joos, F.: Observation-constrained estimates of the global ocean carbon sink from Earth System Models, 19, 4431–4457, <https://doi.org/10.5194/bg-19-4431-2022>, 2022.

610

Terhaar, J., Goris, N., Müller, J. D., DeVries, T., Gruber, N., Hauck, J., Perez, F. F., and Séférian, R.: Assessment of Global Ocean Biogeochemistry Models for Ocean Carbon Sink Estimates in RECCAP2 and Recommendations for Future Studies, *J. Adv. Model. Earth Syst.*, 16, e2023MS003840, <https://doi.org/https://doi.org/10.1029/2023MS003840>, 2024.

615 Tjiputra, J. F., Schwinger, J., Bentsen, M., Morée, A. L., Gao, S., Bethke, I., Heinze, C., Goris, N., Gupta, A., He, Y.-C., Olivié, D., Seland, Ø., and Schulz, M.: Ocean biogeochemistry in the Norwegian Earth System Model version 2 (NorESM2), *Geosci. Model Dev.*, 13, 2393–2431, <https://doi.org/10.5194/gmd-13-2393-2020>, 2020.

Tsujino, H., Urakawa, S., Nakano, H., Small, R. J., Kim, W. M., Yeager, S. G., Danabasoglu, G., Suzuki, T., Bamber, J. L., 620 Bentsen, M., Böning, C. W., Bozec, A., Chassignet, E. P., Curchitser, E., Boeira Dias, F., Durack, P. J., Griffies, S. M., Harada, Y., Ilicak, M., Josey, S. A., Kobayashi, C., Kobayashi, S., Komuro, Y., Large, W. G., Le Sommer, J., Marsland, S. J., Masina, S., Scheinert, M., Tomita, H., Valdivieso, M., and Yamazaki, D.: JRA-55 based surface dataset for driving ocean–sea-ice models (JRA55-do), *Ocean Model.*, 130, 79–139, <https://doi.org/https://doi.org/10.1016/j.ocemod.2018.07.002>, 2018.

625

Urakawa, L. S., Tsujino, H., Nakano, H., Sakamoto, K., Yamanaka, G., and Toyoda, T.: The sensitivity of a depth-coordinate model to diapycnal mixing induced by practical implementations of the isopycnal tracer diffusion scheme, *Ocean Model.*, 154, 101693, <https://doi.org/https://doi.org/10.1016/j.ocemod.2020.101693>, 2020.



- 630 Vaithinada Ayar, P., Bopp, L., Christian, J. R., Ilyina, T., Krasting, J. P., Séférian, R., Tsujino, H., Watanabe, M., Yool, A.,  
and Tjiputra, J.: Contrasting projections of the ENSO-driven CO<sub>2</sub> flux variability in the equatorial Pacific under high-  
warming scenario, *Earth Syst. Dyn.*, 13, 1097–1118, <https://doi.org/10.5194/esd-13-1097-2022>, 2022.
- Watson, A. J., Schuster, U., Shutler, J. D., Holding, T., Ashton, I. G. C., Landschützer, P., Woolf, D. K., and Goddijn-  
635 Murphy, L.: Revised estimates of ocean-atmosphere CO<sub>2</sub> flux are consistent with ocean carbon inventory, *Nat. Commun.*,  
11, 4422, <https://doi.org/10.1038/s41467-020-18203-3>, 2020.
- Wright, R. M., Le Quéré, C., Buitenhuis, E., Pitois, S., and Gibbons, M. J.: Role of jellyfish in the plankton ecosystem  
revealed using a global ocean biogeochemical model, 18, 1291–1320, <https://doi.org/10.5194/bg-18-1291-2021>, 2021.
- 640 Yukimoto, S., Kawai, H., Koshiro, T., Oshima, N., Yoshida, K., Urakawa, S., Tsujino, H., Deushi, M., Tanaka, T., Hosaka,  
M., Yabu, S., Yoshimura, H., Shindo, E., Mizuta, R., Obata, A., Adachi, Y., and Ishii, M.: The Meteorological Research  
Institute Earth System Model Version 2.0, MRI-ESM2.0: Description and Basic Evaluation of the Physical Component, *J.*  
*Meteorol. Soc. Japan. Ser. II*, 97, 931–965, <https://doi.org/10.2151/jmsj.2019-051>, 2019.
- 645 Zeng, J., Iida, Y., Matsunaga, T., and Shirai, T.: Surface ocean CO<sub>2</sub> concentration and air-sea flux estimate by machine  
learning with modelled variable trends, *Front. Mar. Sci.*, 9, 2022.
- Ziehn, T., Chamberlain, M. A., Law, R. M., Lenton, A., Bodman, R. W., Dix, M., Stevens, L., Wang, Y.-P., and Srbinovsky,  
650 J.: The Australian Earth System Model: ACCESS-ESM1.5, *J. South. Hemisph. Earth Syst. Sci.*, 70, 193–214, 2020.